



Direct synthesis of silver/polymer/carbon nanocables via a simple hydrothermal route

Mingshang Jin, Qin Kuang*, Zhiyuan Jiang, Tao Xu, Zhaoxiong Xie*, Lansun Zheng

State Key Laboratory for Physical Chemistry of Solid Surfaces, Department of Chemistry, College of Chemistry and Chemical Engineering, Xiamen University, Xiamen 361005, China

ARTICLE INFO

Article history:

Received 10 March 2008

Received in revised form

19 May 2008

Accepted 21 May 2008

Available online 29 May 2008

Keywords:

Silver

Nanocables

Hydrothermal

Carbonization

ABSTRACT

High-yield silver/polymer/carbon nanocables were synthesized via a one-step simple hydrothermal route by using silver chloride and glucose as precursors. High-resolution TEM and element mapping proved that as-prepared nanocables consist of a silver nanowire core, a polymer inner shell, and a graphitic carbon outer shell. A three-step growth mechanism was proposed to explain the growth of such three-layer nanocables, i.e. the formation of silver nanowires, the glycosidation of glucose molecules on silver nanowire surface and the carbonization of the outmost glycosidation layer. We believe that reaction temperature plays the key role in the polymerization of glucose and sequent surface-carbonization.

© 2008 Elsevier Inc. All rights reserved.

1. Introduction

Among all metals, pure silver possesses the highest electrical and thermal conductivity. Therefore, 1D nanostructures of silver have attracted increasing interest due to their potential applications as building blocks for nanoscale electronic, optoelectronic, and magnetic devices. So far, many 1D silver nanostructures (such as nanowires, nanorods, and nanotubes) have been successfully prepared by means of different synthetic strategies including surfactant-assisted synthesis [1–4], hard template-directed methods [5–10], surfactantless methods [11,12], and electrochemical deposition methods [13,14]. Recently, many efforts have been devoted into the synthesis of a special 1D silver co-axial heterostructures (i.e. the so-called nanocable) through assembling single insulating nanotubes and/or silver nanowires in a radial direction [15–25]. For example, Xia's group synthesized Ag/Si nanocables by directly coating bycrystalline silver nanowires with conformal sheaths of silica by a sol-gel process [15]. Yu's group successfully prepared well-defined silver/PVA sub-microcables by a hydrothermal reaction [16,17]. Other kinds of silver nanocables including silver/PVP, silver/PPy, silver/C, and silver/carbon rich composites have been also synthesized in succession [18–25]. These special 1D nanostructures are anticipated to have potential application in nanoscale electronic devices due to the unique structure composing a high-conductive silver core and an insulating outer shell. Herein, we present a simple hydrothermal

route for the synthesis of silver/polymer/carbon nanocables on a large scale by using glucose as the reductant and silver chloride as the silver source. This kind of three-layer nanocables consists of a silver nanowire as a core, a polymer as an inner shell and a graphitic carbon as an outer shell. Our experiments demonstrate that such three-layer nanocables follow a three-step growth mechanism, i.e. the formation of silver nanowires, the glycosidation of glucose molecules on nanowire surface, and the carbonization of the outmost glycosidation layer. Reaction temperature is thought to be the most crucial factor of these three-layer nanocables.

2. Experimental section

In a typical experiment, 5 mL of 0.1 M AgNO₃ solution, 5 mL of 0.2 M NaCl solution and 10 mL of 0.2 M glucose solution were added to a Teflon-lined autoclave in sequence. The autoclave was heated at 150 °C for 2 days and then cooled naturally in air. The brown product was collected from the suspension by centrifugal separation at 4000 rpm for 5 min and was further cleaned with deionized water and ethanol. The morphology and structure of the products were characterized by X-ray diffraction (XRD, Panalytical X'pert PRO) with Cu K α radiation, field emission scanning electron microscopy (FE-SEM, LEO 1530) and high-resolution transmission electron microscopy (HRTEM, TECNAI F30) with the accelerate voltage of 300 kV. The element mapping was performed using Gatan image filtering (GIF) system attached to F30 HRTEM. For TEM characterization, the products were ultrasonically dispersed

* Corresponding authors. Fax: +86 592 2183047.

E-mail addresses: qkuang@xmu.edu.cn (Q. Kuang), zxjie@xmu.edu.cn (Z. Xie).

into absolute alcohol and dropped on a copper grid coated with carbon film.

3. Results and discussion

Fig. 1A is a typical XRD pattern of as-prepared products, showing the presence of metallic silver. All sharp peaks from left to right can be indexed to diffractions from the {111}, {200}, {220}, and {311} planes of face-centered cubic silver (JCPDS Card File No. 04-0783). We note that there is a broaden peak at about $2\theta = 25^\circ$, which suggests that the products also contain lots of amorphous compounds. Fig. 1B is a high-magnification SEM image of the products. It is found that as-prepared products are of 1D structure like the cables, in which the cores are brighter than the shells. As the materials with heavier atomic mass may reflect much more electrons, the core of these cables should be the metallic silver. More detailed information of these cables is provided by corresponding TEM observation. As shown in Fig. 1C, most cables consist of continuous nanowires with diameter ranging from 50 to 200 nm and shells with thickness ranging from tens of nanometers to hundreds of nanometers. We find that some silver nanowires grows out of the shell as pointed out by the arrow in Fig. 1C and other silver nanowires are completely encapsulated in the shell shown in Fig. 1D. In addition, some cables containing

discontinuous Ag nanowire cores (Fig. 1E) are also observed, and the ratio of them in all products is estimated to be 30%. Interestingly, some nanowire cores cross each other and their surfaces are uniformly covered with a shell (Fig. 1F). Above

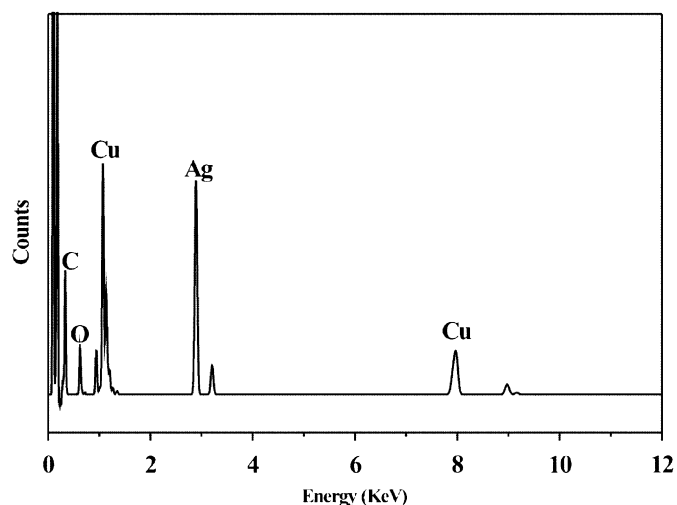


Fig. 2. The EDX spectrum taken from a single silver nanocable.

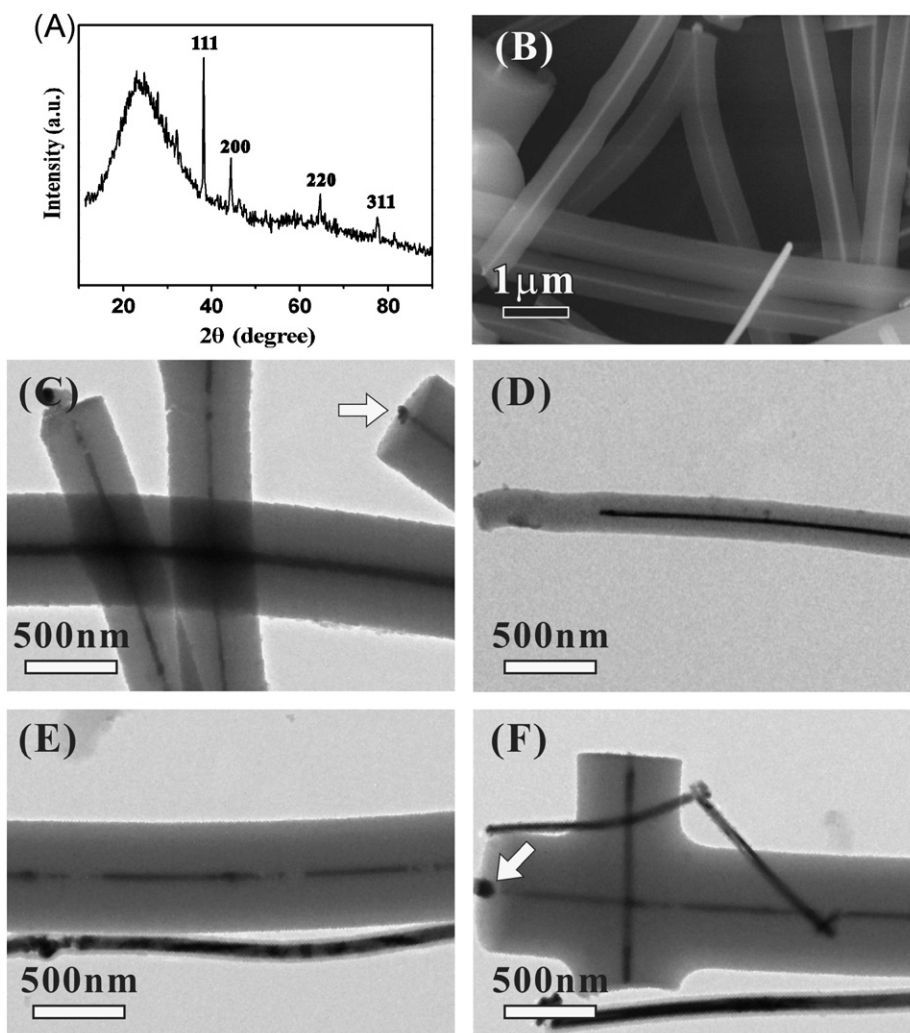


Fig. 1. (A) Typical XRD pattern of as-prepared products at the condition of the molar ratio of 1:2:4 ($\text{Ag}^+:\text{Cl}^-:\text{glucose}$) and the temperature of 150°C for 2 days; (B) corresponding SEM image; and (C)–(F) low-magnification TEM of as-prepared products.

particular cable-like nanostructures provide some useful clue for exploring formation mechanism of silver nanocables, and will be discussed in the later part.

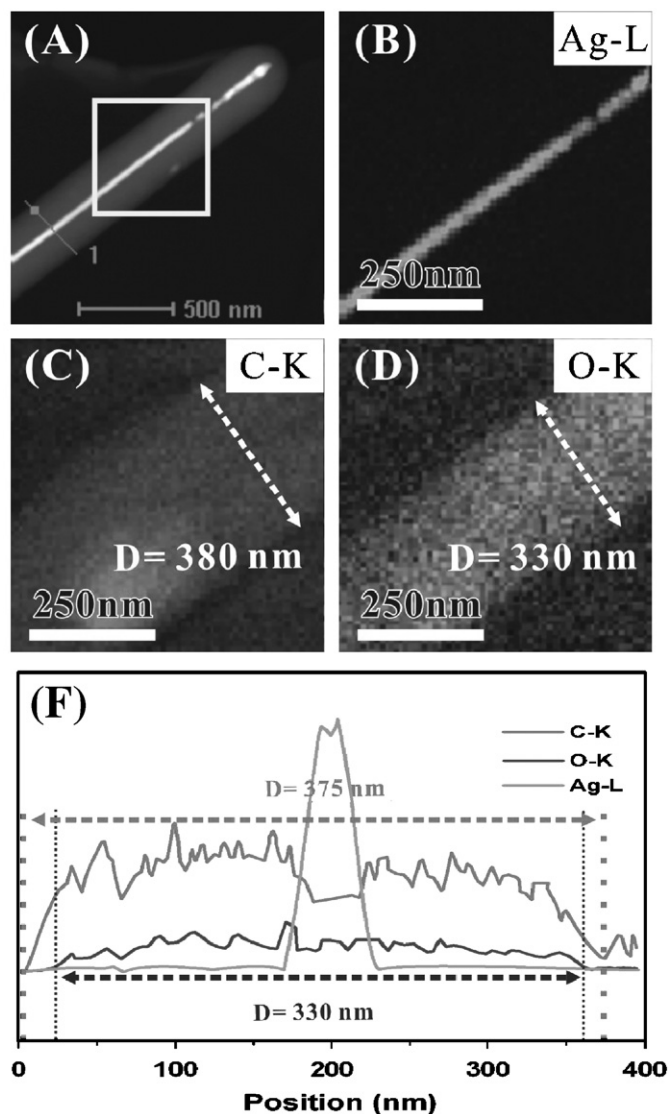


Fig. 3. (A) STEM image of a silver nanocable; (B)–(D) elemental maps of Ag, C, and O concentrations recorded from the area marked by a yellow rectangle in the silver nanocable of (A); and (E) cross-sectional compositional line profiles recorded from the area marked by a red line in the silver nanocable of (A).

The chemical composition of the nanocables is further determined using the energy dispersive X-ray (EDX) spectrum of TEM. As shown in Fig. 2, there are four kinds of peaks in the EDX spectrum taken from a single nanocable, which correspond to elements C, O, Ag, and Cu, respectively. Strong Cu peaks originate from the copper TEM grid that supports the sample, Ag peak should come from silver nanowire core of the cable; O and C peaks should come from the shell of the cable.

In order to confirm the element distribution in the core and shell of the nanocable, scanning transmission electron microscopy (STEM) and the elemental mapping techniques are further carried out. Figs. 3B–D is corresponding elemental maps of Ag, C, and O concentration recorded from the rectangle area of a single nanocable shown in Fig. 3A, respectively. It is clearly seen that the element Ag locates in the core and the elements C and O are uniformly distributed in whole nanocables, which indicates that the core of the nanocable is a silver nanowire and the shell of the nanocable is some organic matters composing elements O and C. Previous studies demonstrated that the polymerization reaction of glucose would take place under appropriate hydrothermal conditions and resulted in the formation of polymer [25–27]. Hence, the shell of the nanocable should be a glycosidation layer formed by polymerization of glucose. In addition, it should be noted that there is a little difference for the distribution area size between the element O and the element C, because the distribution area of the element O is clearly smaller than that of the element C. Analysis of the cross-sectional composition line profiles (Fig. 3E) further confirm the distribution status of these elements, showing that the silver core is about 60 nm in diameter, the C layer is up to 380 nm, but the O layer is only 330 nm. Above results indicate that the element O does not appear at the outmost shell of the cable, and carbonization occurred to a certain extent at the outmost shell of the nanocable.

The microstructures of the as-prepared silver nanocable were investigated by HRTEM and selective area electron diffraction (SAED). Fig. 4A is a low-magnification HRTEM image of a single nanocable where a silver nanowire is completely encapsulated in the surrounding shell. The diameter of this silver nanowire core is about 170 nm and the thickness of its shell is about 280 nm. As shown in Fig. 4B, a SAED pattern recorded from the silver nanowire core can be indexed as two sets of diffractions corresponding to the diffractions of the $[\bar{1}12]$ and the $[001]$ zone axes, respectively. The white solid network in the SAED pattern corresponds to the diffraction of the $[\bar{1}12]$ zone axis, while the white dot network corresponds to the $[001]$ zone diffraction. The two sets of diffraction share a common $[220]$ diffraction, which is the longitudinal direction of the nanocable. This result agrees well with our previous study of pure silver nanowires that were synthesized by simply reducing silver ions with glucose without

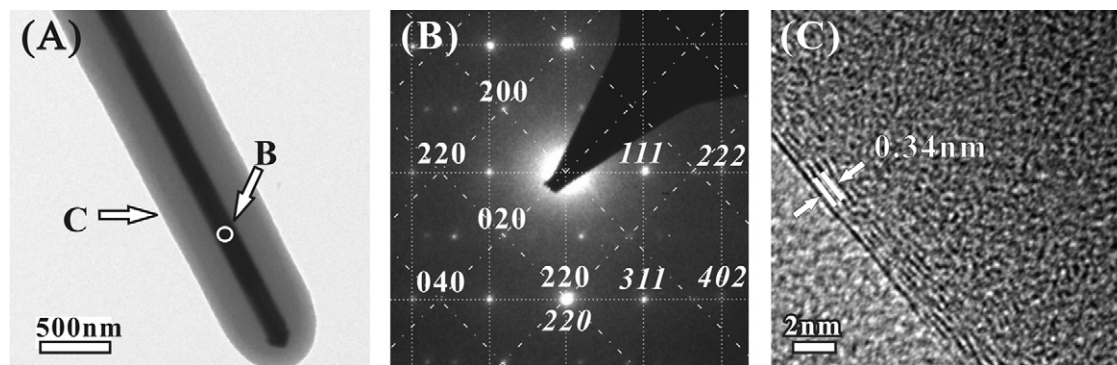


Fig. 4. (A) TEM image of a silver nanocable; (B) corresponding SAED pattern recorded from the nanowire core marked by the arrow “B” in (A); and (C) HRTEM image recorded from outer surface of the silver nanocable, which indicated by the arrow “C” in (A).

the assistance of surfactants or capping reagents [28]. In that case, we proposed a cyclic penta-twinned crystal growth mechanism for the 1D growth of the Ag nanowires. The silver nanowire core of the as-prepared nanocable is also cyclic penta-twinned crystals and as a consequence, follows the same cyclic penta-twinned crystal growth mechanism as pure silver nanowires do. Fig. 4C is a typical HRTEM image taken from the surface of silver nanocable. Obviously, the inner shell is amorphous because no ordered lattice can be observed, which reasonably accounts for the appearance of a broad peak at $2\theta = 25^\circ$ in XRD characterization shown in Fig. 1A. However, the outer shell clearly exhibits ordered fringes with lattice spacing of 0.34 nm, which is in accordance with the standard lattice spacing of graphitic carbon. Above results, combining with the XRD pattern and elemental mapping results, demonstrate unambiguously that the inner shell of the nanocable is the product of polymerization of glucose while the outermost shell has been completely carbonized into graphite.

To further investigate the mechanism of the formation of the polymer and graphitic carbon shell, the products of the earlier reaction stage are observed. Fig. 5 shows the products picked up from the same reactant but with relatively short the reaction time (for 12 h). It can be seen that the silver nanowires have been well grown, but the surrounding sheaths cannot be clearly found around silver nanowires. From this experiment, we can conclude that the silver nanowires form first during the reaction, and then polymerization of glucose occurs on the silver nanowires. Because the reductant glucose molecules are able to adsorb on the nanowire surfaces, they factually play the role of surfactants during the growth of silver penta-twinned nanowires [28]. At the same time, the adsorbed glucose on the Ag nanowires' surface might act as starting point for the polymerization of glucose. This

hypothesis could well explain the formation of the some cross-linked cables shown in Fig. 1F because the growth of such cross-linked cables can be thought as that the pre-formed nanowires occasionally touch together, and then the shells uniformly grow on them.

Combining all the information discussed above, a growth mechanism of the Ag/polymer/carbon cable is proposed as shown in the schematic diagram of Fig. 6. Firstly, silver ions released from the AgCl particles are gradually reduced and grows into the silver nanowires via a cyclic penta-twinned growth mechanism. Then the adsorbed glucose molecules on the silver nanowire surfaces act as nucleation sites for the glycosidation, resulting in the formation of polymer layer on the silver nanowire surface. In the final step, partial carbonization occurs and results in the formation of the thin graphitic carbon layer on the nanocable surface.

The proposed formation mechanism of Ag/polymer/carbon in this paper is different from previous proposed formation mechanism that polymerization and carbonization of glucose occurred with the development of silver nanowires simultaneously [16,24]. Reaction temperature is believed to be the crucial factor, which has a great influence on the formation process of Ag nanowires and polymer/carbon shell. Previous studies have demonstrated that under the hydrothermal condition, it has been found that polymerization of glucose (i.e. glycosidation) occurs at relatively low temperature ($\sim 140^\circ\text{C}$) while aromatization and carbonization occurs at the temperature over 160°C [24–27]. As typical examples, Li's group successfully prepared high-purity carbon spheres and cylindrical silver nanocables with carbon shell by controlling different reaction temperature from 160 to 180°C [25,26]. In our experiment, the reaction temperature is controlled to 150°C , a little higher than the reported critical temperature (140°C) of polymerization reaction and a little lower than the reported critical temperature (160°C) of carbonization reaction. Therefore, it is reasonable to believe that carbonization occurs at 150°C , but with very low reaction rate. Furthermore, the carbonization should start from the surface of the glycosidation layer because graphitic carbon only appears on the out-most layer of the shell.

4. Conclusions

In conclusion, silver core/multishell nanocables, consisting of a silver nanowire core, a polymer inner shell and a graphitic carbon outer shell have been successfully synthesized via a simple one-step hydrothermal reaction from the solution containing AgCl and glucose. It is found that glycosidation easily occurs on the silver nanowire surfaces, resulting in the formation of complicated cross-linked cables. Furthermore, carbonization starts from outer surface of the polymer layer, rather than from the surface of silver nanowires, indicating that silver nanowires do not act as catalysts during the carbonization.

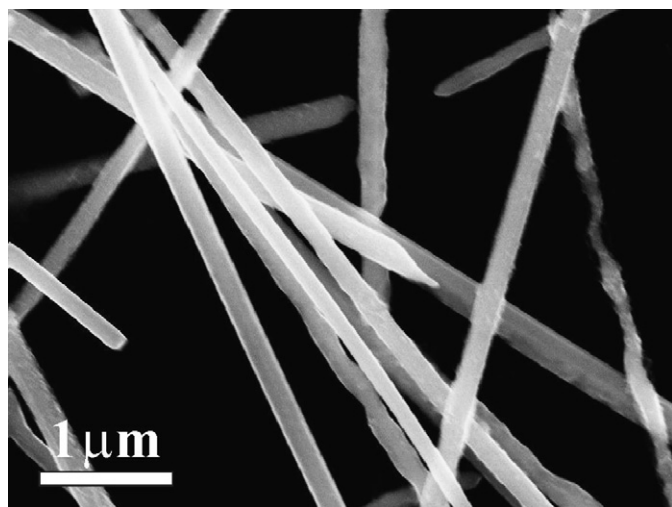


Fig. 5. SEM image of silver nanocables synthesized at 150°C for 12 h.

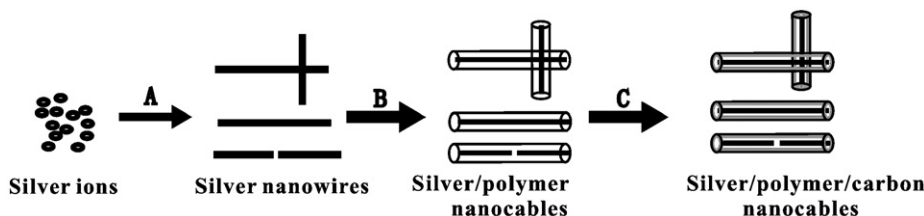


Fig. 6. Schematic illustration of the growth mechanism of the three-layered nanocables. (A) Silver ions release from the AgCl particles and are reduced to the silver nanowires; (B) the adsorbed glucose molecules on the silver nanowire surfaces act as nucleation sites for the glycosidation, resulting in the formation of polymer layer on the silver nanowire surface; and (C) carbonization occurs and results in the formation of the thin graphitic carbon layer on the nanocable surface.

Acknowledgments

This work was supported by the National Natural Science Foundation of China (Grant nos. 20725310, 20721001, 20673085, and 20671078), the National Basic Research Program of China (Grant no. 2007CB815303), Key Scientific Project of Fujian Province of China (Grant no. 2005HZ01-3).

References

- [1] Y.G. Sun, B. Mayers, T. Herricks, Y.N. Xia, *Nano Lett.* 2 (2002) 165–168.
- [2] Y.G. Sun, Y.N. Xia, *Adv. Mater.* 14 (2002) 833–837.
- [3] N.R. Jana, L. Gearheart, C.J. Murphy, *Chem. Commun.* (2001) 617–618.
- [4] J.Q. Hu, Q. Chen, Z.X. Xie, G.B. Han, R.H. Wang, B. Ren, Y. Zhang, Z.L. Yang, Z.Q. Tian, *Adv. Funct. Mater.* 14 (2004) 183–189.
- [5] R. Yang, C.H. Sui, J. Gong, L.Y. Qu, *Mater. Lett.* 61 (2007) 900–903.
- [6] M.H. Huang, A. Choudrey, P.D. Yang, *Chem. Commun.* (2000) 1063–1064.
- [7] Y.J. Han, J.M. Kim, G.D. Stucky, *Chem. Mater.* 12 (2000) 2068–2069.
- [8] J. Sloan, D.M. Wright, H.G. Woo, S. Bailey, G. Brown, A.P.E. York, K.S. Coleman, J.L. Hutchison, M.L.H. Green, *Chem. Commun.* (1999) 699–700.
- [9] A. Govindaraj, B.C. Satishkumar, M. Nath, C.N.R. Rao, *Chem. Mater.* 12 (2000) 202–205.
- [10] P. Gao, C.L. Zhan, M.H. Liu, *Langmuir* 22 (2006) 775–779.
- [11] Z.H. Wang, J.N. Liu, X.Y. Chen, J.X. Wan, Y.T. Qian, *Chem. Eur. J.* 11 (2005) 160–163.
- [12] K.K. Caswell, C.M. Bender, C.J. Murphy, *Nano Lett.* 3 (2003) 667–669.
- [13] M. Mazur, *Electrochem. Commun.* 6 (2003) 400–403.
- [14] X.J. Zheng, Z.Y. Jiang, Z.X. Xie, S.H. Zhang, B.W. Mao, L.S. Zheng, *Electrochem. Commun.* 9 (2007) 629–632.
- [15] Y.D. Yin, Y. Lu, Y.G. Sun, Y.N. Xia, *Nano Lett.* 2 (2002) 427–430.
- [16] L.B. Luo, S.H. Yu, H.S. Qian, T. Zhou, *J. Am. Chem. Soc.* 127 (2005) 2822–2823.
- [17] L.B. Luo, S.H. Yu, H.S. Qian, J.Y. Gong, *Chem. Commun.* (2006) 793–795.
- [18] K. Zou, X.H. Zhang, X.F. Duan, X.M. Meng, S.K. Wu, *J. Cryst. Growth* 273 (2004) 285–291.
- [19] J.C. Yu, X.L. Hu, L.B. Quan, L.Z. Zhang, *Chem. Commun.* (2005) 2704–2706.
- [20] W.Z. Wang, S.L. Xiong, L.Y. Chen, B.J. Xi, H.Y. Zhou, Z.D. Zhang, *Cryst. Growth Des.* 6 (2006) 2422–2426.
- [21] A.H. Chen, K. Kamata, M. Nakagawa, T. Iyoda, H.Q. Wang, X.Y. Li, *J. Phys. Chem. B* 109 (2005) 18283–18288.
- [22] A.H. Chen, H.Q. Wang, X.Y. Li, *Chem. Commun.* (2005) 1863–1864.
- [23] Z. Fang, K.B. Tang, S.J. Lei, T.W. Li, *Nanotechnology* 17 (2006) 3008–3011.
- [24] S.H. Yu, X.J. Cui, L.L. Li, K. Li, B. Yu, M. Antonietti, H. Colfen, *Adv. Mater.* 16 (2004) 1636–1640.
- [25] X.M. Sun, Y.D. Li, *Adv. Mater.* 17 (2005) 2626–2630.
- [26] X.M. Sun, Y.D. Li, *Angew. Chem. Int. Ed.* 43 (2004) 597–601.
- [27] H.S. Qian, S.H. Yu, L.B. Luo, J.Y. Gong, L.F. Fei, X.M. Liu, *Chem. Mater.* 18 (2006) 2101–2108.
- [28] S.H. Zhang, Z.Y. Jiang, Z.X. Xie, X. Xu, R.B. Huang, L.S. Zheng, *J. Phys. Chem. B* 109 (2005) 9416–9421.